Expression analysis of *Dickkopf-related protein 3* (*Dkk3*) suggests its pleiotropic roles for a secretory glycoprotein in adult mouse

Junji Inoue[1] ▪ Hirofumi Fujita[1] ▪ Tetsuya Bando[1] ▪ Yoichi Kondo[1,†] ▪ Hiromi Kumon[2,3] ▪ Hideyo Ohuchi[1]

[1] Department of Cytology and Histology, Okayama University Graduate School of Medicine, Dentistry and Pharmaceutical Sciences, 2-5-1 Shikata-cho, Kita-ku, Okayama 700-8558, Japan

[2] Innovation Center Okayama for Nanobio-targeted Therapy (ICONT), Okayama University, 2-5-1 Shikata-cho, Kita-ku, Okayama 700-8558, Japan

[3] Niimi College, 1263-2 Nishigata, Niimi, Okayama 718-8585, Japan

Correspondence to: Hideyo Ohuchi, Department of Cytology and Histology, Okayama University Graduate School of Medicine, Dentistry and Pharmaceutical Sciences, Okayama 700-8558, Japan. E-mail: hohuchi@okayama-u.ac.jp

[†] Present Address: Department of Anatomy, Osaka Medical College, 2-7 Daigaku-cho, Takatsuki, 569-8686, Japan

Abstract

Dickkopf-related protein 3 (*Dkk3*) is the third member of the *Dkk* gene family and identical to the gene, whose expression was reduced in immortalized cells. Therefore, its another name is *reduced expression in immortalized cells (REIC)*. Since the intratumoral introduction of *Dkk3* inhibits tumor growth in mouse models of cancers, *Dkk3* is likely a tumor suppressor gene. However, the functions of *Dkk3 in vivo* remain unclear. As the first step to decipher the physiological roles of this gene, we examined the expression pattern of *Dkk3* in various tissues from adult mice. *In situ* hybridization showed that *Dkk3* mRNA was detected in the brain, retina, heart, gastrointestinal tract, adrenal glands, thymus, prostate glands, seminal vesicles, testes, and ovaries in a regionally specific manner. Furthermore, we raised anti-mouse Dkk3 antibody and performed immunohistochemistry. Cytoplasmic localization of Dkk3 protein was observed in the cells of the adrenal medulla, while Dkk3 immunoreactivity was observed in the lumen of the stomach and intestine, implying that the Dkk3 protein may be secreted into the lumen of the gastrointestinal tract. These results suggest that *Dkk3* has pleiotropic roles for a secretory glycoprotein that acts primarily in the gastrointestinal tract, thymus, endocrine and reproductive organs of the mouse.

Keywords Dkk3 ▪ REIC ▪ *in situ* hybridization ▪ immunohistochemistry ▪ mouse

Introduction

The *Dickkopf-related protein 3* (*Dkk3*) gene is a member of the *Dkk* gene family, which comprises five members: *Dkk1* through *Dkk4*, and *Dkk like 1* (*Dkkl1* or *Soggy1*). This gene family name stems from the ability of its founding member, Dkk1, to induce head formation in *Xenopus* embryos (Glinka et al 1998). Dkk proteins are secretory glycoproteins that contain an N-terminal signal peptide. In addition, all Dkk proteins, except Dkkl1, have two conserved cysteine-rich domains, although the exact functions of these domains remain elusive. The overall amino acid sequence homology between Dkk3 and the other Dkk proteins ranges from 37-40%, and this is less than the homology between Dkk1, Dkk2, and Dkk4 (46-50%) (Krupnik et al 1999). Accordingly, Dkk1, Dkk2, and Dkk4 have been shown to antagonize Wnt-mediated β-catenin stabilization by binding to Wnt co-receptors (Bafico et al 2001; Mao and Niehrs 2003; Niehrs 2006). In contrast, Dkk3 does not bind the co-receptors at the cell surface membrane (Veeck and Dahl 2012; Fujii et al 2014), although it downregulates Wnt/β-catenin signaling in mouse testis (Das et al 2013) and human cancers (Lee et al 2009; Veeck et al 2009; Xiang et al 2013; Hara et al 2015; Wang et al 2015).

Another aspect of Dkk3 is having a potential for the tumor suppressor. The human *Dkk3* gene exhibits reduced expression in immortalized cells (Tsuji et al 2000),

and thus is called *REIC*. Consistently, *Dkk3* expression is reduced in a broad range of human cancers (Veeck and Dahl 2012). Based on these findings, *Dkk3* reexpression strategies have been attempted as a cancer therapy. Overexpression of human *Dkk3*/*REIC* gene induces apoptosis in prostate and testicular cancers, but not in normal cells (Abarzua et al 2005; Tanimoto et al 2007). The mechanisms for this tumor-specific apoptosis have been elucidated as through endoplasmic reticulum (ER) stress, activation of c-Jun-NH2-kinase (Abarzua et al 2005; Tanimoto et al 2010) or anticancer immune responses by inducing the formation of dendritic cells (Watanabe et al 2009).

A number of studies has been clarified the *Dkk3* expression pattern in embryonic and adult normal tissues. During mouse development, transcription of the *Dkk* genes is temporally and spatially regulated with overlapping expression domains, suggesting their involvement in interactions between epithelial and mesenchymal cells (Monaghan et al 1999). In adult murine tissues, *Dkk3* mRNA has been detected in brain, eye, heart, lung, ovary, skeletal muscle, and uterus with reverse transcription PCR analysis (Monaghan et al 1999). In human tissues, *Dkk3* is expressed in the placenta, pancreas, adrenal, trachea, spinal cord, thyroid, and stomach, as well as in the brain and heart according to Northern blot analysis (Krupnik et al 1999). However, detailed localization studies for *Dkk3* mRNA or protein within tissues are quite limited (Krupnik

et al 1999; Du et al 2011; Kataoka et al 2012), and *Dkk3* knockout mice are viable without apparently deteriorate phenotypes (Barrantes et al 2006), which remained to be further analyzed. As the first step to decipher the physiological roles for Dkk3, here we examined the expression pattern of *Dkk-3* in various tissues from adult mice by *in situ* hybridization (ISH) and immunohistochemistry.

Material and methods

Animals

All animal care and experiments were carried out in accordance with the Guidelines for Animal Experiments of Okayama University, and were approved by the Ethics Committee of Okayama University for Animal Research (approval numbers: OKU-2013189, OKU-2013270, and OKU-2014106). Organs were obtained from male and female C57BL/6 or 129S6 mice (ranging in age from 10–25 weeks). Each experiment was performed at least in duplicate and using at least two individual animals. The mice were housed in separate cages and had access to food and water *ad libitum*. Histology evaluations were performed with hematoxylin-eosin staining (not shown). Tissues from *Dkk3* knockout (*Dkk3*$^{-/-}$) mice (129S6/SvEvTacDkk3<tm1Tfur>, RBRC02847, Riken Bioresource Center, Tsukuba, Japan) deposited by Dr. Takahisa Furukawa (Institute for Protein Research, Osaka University) were used as negative controls in both immunohistochemistry and Western blot analyses.

Frozen sections

Mice were fixed with 4% paraformaldehyde (PFA)/phosphate buffered saline (PBS) via transcardial perfusion. Subsequently, tissues were collected and fixed in 4% PFA/PBS

on ice for 6 h, then equilibrated in PBS containing 15% sucrose until the tissues sank down. After an overnight incubation in PBS containing 30% sucrose, the fixed tissues were embedded in optimal cutting temperature compound (Sakura Finetek Japan, Tokyo, Japan). After the embedded tissues were frozen in a dry-ice cooled ethanol bath, the frozen blocks were sectioned (14 μm) with a cryostat. The tissue sections were stored at -20°C until further use.

ISH

Riboprobes for ISH were synthesized by *in vitro* transcription using the coding region of the mouse *Dkk3* cDNA (1047 base pairs, encoding 349 amino acids) as a template and T7 or T3 RNA polymerase (Roche, Basel, Switzerland). The ISH was performed essentially as reported previously (Schaeren-Wiemers and Gerfin-Moser 1993). Briefly, mouse organ sections were thawed, air dried, fixed with 4% PFA/PBS, and treated with 8 μg/ml proteinase K (Roche) at room temperature (RT). After 10 min, the sections were fixed with 4% PFA/PBS for an additional 10 min before being incubated in an acetylation solution (1.2% triethanolamine [Sigma-Aldrich, St. Louis, MO] /0.25% acetic acid [Wako Pure Chemical Industries, Osaka, Japan]). After 10 min, the sections were incubated with hybridization buffer (50% formamide [Wako], 5× saline-sodium

citrate [SSC] buffer, 5× Denhardt's solution [Sigma], 250 μg/ml baker's yeast RNA [Sigma], and 500 μg/ml herring sperm DNA [Sigma]) at 72 °C for 3 h. Subsequently, the sections were incubated with hybridization buffer containing digoxigenin-labeled RNA probes at 72 °C overnight. The following day, the sections were washed with 0.2× SSC buffer. Hybridization signals were detected with an alkaline phosphatase-conjugated antibody (Roche) and a solution of nitro-blue tetrazolium and 5-bromo-4-chloro-3'-indolyphosphate (Roche). Tris-EDTA buffer (pH 9.5) was used to stop the staining reaction. Micrograph images were taken with a DS-Ri1 digital camera (Nikon, Tokyo, Japan) equipped with a DM5000B microscopy (Leica Microsystems, Wetzlar, Germany) and processed using Adobe Photoshop CS 5.1 (Adobe Systems, San Jose, CA).

Antibody production

Recombinant full-length mouse Dkk3 protein was synthesized in *E. coli,* purified, and used for the immunization of New Zealand white rabbits (Medical and Biological Laboratories, Nagoya, Japan). IgG fractions were purified from serum samples collected from the rabbits by ammonium sulfate precipitation followed by caprylic acid precipitation (Momotaro-Gene Inc., Okayama, Japan).

Western blotting

Adult (11 weeks) male mice were anesthetized and perfused with ice-cold PBS before tissues were resected and frozen in liquid nitrogen. After the frozen tissues were pulverized with a hammer at -20 °C, they were solubilized in ice-cold lysis buffer (10 mM Tris-HCl [pH 7.4], 0.15 M NaCl, 1% nonylphenoxypolyethoxylethanol, 0.1% sodium dodecyl sulfate [SDS], 0.1% sodium deoxycholate, 1 mM EDTA, 1 mM phenylmethylsulfonyl fluoride, 1 μg/ml leupeptin, and 5 μg/ml pepstatin A). Total protein (50 μ g each) from brain, eye, heart, stomach, adrenal glands, skin, testis, and spleen extracts collected from wild-type and *Dkk3*$^{-/-}$ mice (Fig. 5), was denatured by heating for 5 min at 95 °C with sample buffer containing β-mercaptoethanol. The denatured proteins were subjected to 10% SDS-polyacrylamide gel electrophoresis and then transferred electrophoretically onto polyvinylidene difluoride (PVDF) membranes (Millipore, Waltham, MA). The membranes were subsequently incubated with anti-mouse Dkk3 antibody (diluted 1:10,000) or anti-Cyclophilin B antibody (Cell Signaling Technology [CST], Danvers, MA) (diluted 1:1000) at 4 °C overnight. After the membranes were washed, they were incubated with a horseradish peroxidase-conjugated goat anti-rabbit IgG (CST) (diluted 1:5000) at RT for 1.5 h. All

antibodies were diluted in Immunoshot reagent (Cosmo Bio, Tokyo, Japan). Immunoreactive bands were visualized with Immunostar LD reagent (Wako) and a C-DiGit Blot Scanner (LI-COR, Lincoln, NE). The PVDF membranes were stained with Coomassie Brilliant Blue (CBB) for protein detection. Preliminary data showed that the antibody detected a heterogeneous set of bands in mouse wild-type heart and brain extracts, but not in the wild-type liver or in the equivalent tissues obtained from *Dkk3*$^{-/-}$ mice (data not shown).

Immunohistochemistry

Tissue sections were incubated with PBS containing 0.25% Triton X-100 (PBST) 3 times for 5 min each at RT. The sections were then incubated with blocking reagent (PBST containing 5% normal goat serum) for 1 h, followed by an appropriate primary antibody diluted in blocking reagent for 3 h at RT and then overnight at 4 °C. The antibodies used are listed in Table S1. The next day, the sections were rinsed with PBST and incubated with Alexa Fluor 488-conjugated or Alexa Fluor 568-conjugated secondary antibodies (Thermo Fisher Scientific, Waltham, MA) at RT for 1.5 h. After the sections were washed, they were mounted with Vectashield containing 4', 6-diamidino-2-phenylindole (DAPI) (Vector Laboratories, Cambridgeshire, UK). To

visualize mucous neck cells of the stomach, Alexa Fluor 594-conjugated lectin *Griffonia simplicifolia*-II (GSII) (Thermo Fisher Scientific) was used at a concentration of 1 μg/ml. We collected fluorescent images using a LSM 780 confocal laser-scanning microscope (Carl Zeiss Microscopy, Jena, Germany) (Figs. 6 and 7) or a BZ-X700 fluorescence microscope (Keyence, Osaka, Japan) (Fig. S6). In addition to corresponding tissues from *Dkk3*$^{-/-}$mice, normal rabbit IgG (Vector) was used at a concentration of 1 μg/ml as negative controls (Fig. S6).

Results and discussion

Our ISH results showed that the tissue or cell-specific expression pattern of *Dkk3* was observed in the brain, retina, and heart as reported previously (Supplementary Figs. S1 and S2) (Krupnik et al 1999; Barrantes et al 2005). In the cerebellum, we found that *Dkk3* was expressed by Purkinje cells (Fig. S1c-f). This study has further clarified spatial expression domains of *Dkk3* at the mRNA and/or protein level in the gastrointestinal tract (Figs. 1 and 2), adrenal glands (Fig. S3i-o), thymus (Fig. 3e-h), testes (Fig. 4a-f), prostate glands (Fig. 4g-i and Fig. S5), seminal vesicles (Fig. 4j-l), and ovaries (Fig. 4m-o) of the adult mouse as described below.

Digestive organs

In the longitudinal sections of the stomach plus anterior duodenum, *Dkk3* mRNA was detected in the simple columnar epithelium and more intensely in the duodenum (Fig. 1a,b). *Dkk3* was expressed in the mucosa, more specifically, the epithelium of the forestomach (Fig. 1c-f), the gastric corpus (Fig. 1g-m) and the pylorus (Fig. 1n-q). In the gastric corpus, more intense signals for *Dkk3* mRNA were observed in the cells below GSII-positive neck mucous cells, that is, in the chief cell layer (Fig. 1k-m). In the pylorus, more intense signals for *Dkk3* mRNA were observed in the pyloric glands (Fig.

1n-q). In the duodenum, *Dkk3* is abundantly expressed in the columnar epithelial cells and Brunner's glands (Fig. 1r-u). In the gallbladder, *Dkk3* was intensely expressed in the mucosa, while weaker expression of *Dkk3* mRNA was observed in the muscle layer of the gallbladder (Fig. 2a-d). The *Dkk3* mRNA signals in the gastrointestinal mucosa gradually weakened from the intestine toward the rectum (Fig. 2e-p). The submandibular gland and the liver showed no detectable signals for *Dkk3* mRNA (Fig. S4a-h). It was reported that expression of *Dkk3* mRNA was detected in human deep gastric glands and colon (Byun et al 2005). This study has illuminated the broader domain of *Dkk3* expression throughout the gastrointestinal tract and the gallbladder in the mouse.

Endocrine and lymphatic organs

Relatively low level of *Dkk3* expression was observed in follicular epithelial cells of the thyroid gland (Fig. S3a, b), compared with the control result obtained by the sense probe (Fig. S3c, d). In the pancreas, the acinar cells rather than islet cells weakly expressed *Dkk3* mRNA (Fig. S3e-h). The medulla of the adrenal glands expressed higher amount of *Dkk3* mRNA than the cortex, as reported for human (Fig. S3i-l) (Suwa et al 2003). Immunolabeling after ISH showed that *Dkk3*-expressing cells were less

positive for Phenylethanolamine N-methyltransferase (PNMT), the enzyme that converts noradrenaline to adrenaline in the adrenal medulla (Fig. S3m-o). In the lymphatic organs, patchy patterns of *Dkk3* expression were observed in the spleen, which appeared to be unrelated to the red/white pulp structure (Fig. 3a-d). In the thymus, distinct expression of *Dkk3* was detected in the medulla (Fig. 3e-h). The lymph nodes exhibited diffuse expression of *Dkk3* mRNA (Fig. 3i-l). A previous study has shown that Dkk3 has a crucial role in CD8 T cell tolerance (Papatriantafyllou et al 2012). Localization of *Dkk3* mRNA in the thymic medulla may correlate with the role of Dkk3 in T cell tolerance.

Male and female reproductive organs

In the testis, positive signals for *Dkk3* mRNA were observed in cells on the basal side of the seminiferous tubule (Fig. 4a-c). It was reported that *Dkk3* mRNA is expressed in primate testicular Sertoli cells as revealed by PCR analysis (Das et al 2013). However, in the mouse, *Dkk3*-expressing cells were not immunoreactive against Vimentin, a Sertoli cell marker (Fig. 4d-f). Thus, *Dkk3* is expressed by spermatogenic cells such as spermatocytes in the mouse seminiferous tubule.

The mouse prostate glands are composed of three portions, the anterior

(coagulating), dorsal, and ventral glands. In the dorsal prostate gland (Fig. 4g-I, Fig. S5a-d) and seminal vesicle (Fig. 4j-l), intense expression of *Dkk3* mRNA was observed in the epithelium facing the lumen. In contrast, the expression signal for *Dkk3* mRNA was extremely weak in the ventral prostate gland (Fig. S5e-h). Moderate level of *Dkk3* expression was observed in the anterior prostate gland (Fig. S5i-l). The morphology of the dorsal prostate is similar to that of the human prostate, while the anterior prostate and seminal vesicles have similar histological features in the mouse. It is tempting to speculate that the expression of *Dkk3* is related to the maintenance and integrity of epithelial cells of the accessory genital glands in males.

In female mice, intense signals for *Dkk3* mRNA were observed in the ovarian follicular cells and the granulosa cells (Fig. 4m-o), which produce estrogens and contribute to follicle maturation. Furthermore, the epithelium of the uterus moderately expressed *Dkk3* mRNA (Fig. 4p-r), while no signal was detected in the vagina (data not shown).

Respiratory and urinary organs

In these organs, we could not detect obvious *Dkk3* expression (Fig. S4i-x). In the lung, very weak expression of *Dkk3* mRNA was observed in the epithelial cells facing the

pulmonary alveolus (Fig. S4i-l), while a distinct *Dkk3* mRNA signal was not detected in the cells of the trachea (Fig. S4m-p). When the kidney (Fig. S4q-t) and bladder (Fig. S4u-x) were examined, neither organ exhibited a definitively positive signal for *Dkk3* mRNA.

Verification of anti-Dkk3 antibody

To determine localization of Dkk3 protein *in vivo*, immunostaining assays were performed with an antibody raised against recombinant full-length mouse Dkk3 protein. Initially, we examined whether the anti-mouse Dkk3 antibody to be used would detect the expected molecular weight of Dkk3 protein in a Western blot assay. Previously, it was reported that secretion of a Dkk3 protein from HEK293T cells transfected with human *Dkk3* (encoding 350 amino acids) migrated as a heterogeneous set of bands that ranged from 45 to 65 kDa due to post-translational N-glycosylation modifications (Krupnik et al 1999). In our Western blot assays, the antibody used detected a heterogeneous set of bands ranging in size from 38 to 65 kDa in mouse wild-type brain, eye, heart, stomach, adrenal, and skin extracts (Fig. 5). The same bands were essentially not detected in the equivalent tissues obtained from *Dkk3*$^{-/-}$ mice (Fig. 5). However, in testis and spleen, multiple bands were also detected in the extracts from *Dkk3*$^{-/-}$ mice.

Accordingly, when this polyclonal antibody was used in immunohistochemistry assays, a considerable amount of fluorescence signals was observed in sections of testis and spleen from the KO mice (data not shown), indicating that the antibody detected proteins other than Dkk3 as well in these organs. Therefore, in this study, tissues with distinct expression domains of *Dkk3* mRNA were subjected to immunostaining and the corresponding tissues from *Dkk3* KO mice served as negative controls.

Immunohistochemistry

In the brain, fluorescence signals indicating Dkk3 immunoreactivity were observed in the hippocampus (Fig. 6a, b) and cerebral cortex (Fig. 6e, f), which is consistent with the ISH results obtained. In the retina, the ganglion cell layer, the inner nuclear layer, and layer of rods and cones were found to distinctly express Dkk3 protein (Fig. 6i, g). In the heart, Dkk3 immunoreactivity was abundantly observed in the atrium and slightly in the ventricles (Fig. 6m, n). These signals were not observed when control rabbit IgG was used instead of the anti-Dkk3 antibody (Fig. S6) or when *Dkk3*$^{-/-}$ tissues were processed (Fig. 6, third and fourth columns).

In the adrenal gland, distinct Dkk3 immunoreactivity was observed in the medulla that was labeled with an anti-tyrosine hydroxylase antibody (Fig. 6q-t). In

contrast, no fluorescence was observed in the cortex, where low levels of *Dkk3* mRNA expression were detected. A similar localization pattern for *Dkk3* mRNA and protein has been reported in human adrenal glands (Suwa et al 2003). We further found that Dkk3 protein exhibited cytoplasmic localization in cells of the adrenal medulla (Fig. 6r). It is thought that the signal peptide of Dkk3 protein usually mediates its extracellular secretion via the ER-Golgi pathway in response to certain signals. However, Dkk3 also interacts with the intracellular dynein light chain molecule, Tctex-1 (Ochiai et al 2011). Thus, it will be intriguing to elucidate the signals that regulate the secretion of Dkk3 protein from adrenal medulla cells. These results, together with the observed expression of Dkk3 in the atrium (Fig. 6m), which is an endocrine tissue of heart that secretes atrial natriuretic peptide, suggest that Dkk3 has some endocrine-related roles in the mouse.

In the stomach (Fig. 7a,b), Dkk3 protein was localized to the mucosa of the forestomach (Fig. 7c-f) and of the gastric corpus (Fig. 7g-j), which is consistent with the expression domains of *Dkk3* mRNA. In contrast, no clear fluorescence signal was detected in the mucosa of the pylorus (Fig. 7k-n). In the lumen of the stomach and intestine, significant immunoreactivity to the anti-Dkk3 antibody was observed (Fig. 7a,b,o-r). This signal was not detected when control rabbit IgG was used instead of the anti-Dkk3 antibody (Fig. S6) or when *Dkk3*$^{-/-}$ tissues were processed (Fig. 7, panel b and

third and fourth columns). We might have observed localization of Dkk3 protein after its section into the lumen of the gastrointestinal tract in the case of the pylorus and intestine. One explanation is that Dkk3 protein is secreted or released together with sloughed cells into the lumen of the stomach and intestine. Thus, Dkk3 protein may function as a component of digestive juices and tract mucus, which awaits further elucidation.

Since we did not succeed in ISH for skin sections because of the high temperatures needed for hybridization, the skin sections were only subjected to immunohistochemistry. A positive fluorescence signal for Dkk3 protein was observed in both the epidermis and the hair follicles (Fig. 7t), which is consistent with previous findings (Du et al 2011, Kataoka et al 2012). In addition, striated fluorescence signals corresponding to the subcutaneous muscle, *panniculus carnosus*, were detected (Fig. 7u). This muscle is found in the skin of rodents and only in restricted regions of human skin (Bamberger 2005). Dkk3 protein was also detected in the muscularis externa of the forestomach and gastric corpus (Fig. 7c, g). Expression in various muscles including skeletal muscle (Krupnik et al 1999; Veeck and Dahl 2012) is one characteristic for Dkk3.

In summary, this study has clarified new domains of *Dkk3* expression at mRNA and protein level: *Dkk3* mRNA is detected in the epithelial and glandular cells of the gastrointestinal tracts, the gallbladder epithelium, the medulla of thymus, spermatogenic cells of the testis, follicular and granulosa cells of the ovary, and epithelial cells of the prostate, seminal vesicle, and uterus. We raised a polyclonal antibody to the full length of mouse Dkk3 protein. Localization of Dkk3 protein could be specifically detected in the hippocampus, cerebral cortex, retina, and heart, which is consistent to the expression domain of *Dkk3* mRNA. In the gastrointestinal tract, Dkk3 protein may be secreted or released together with sloughed cells into the lumen of the stomach and intestine. Since Dkk3 is a secretory glycoprotein as previously shown *in vitro*, possible roles for Dkk3 in digestive juices and/or tract mucus are suggested. In the adrenal gland, Dkk3 protein is localized to the cytoplasm of the medulla cells, suggesting that Dkk3 protein may be retained within the cell until an appropriate extracellular signal triggers release. Application of Dkk3, or REIC has recently been used for gene therapy to treat human cancers; however, the results shown here would help to open up a new avenue for therapeutics against cancer-unrelated diseases utilizing a secretory protein, Dkk3.

Conflict of Interest: The authors declare that they have no conflict of interest.

Acknowledgements

The authors thank Professor Takahisa Furukawa (Osaka University) for his permission to use the *Dkk3* KO mouse. This study was supported by a grant for Promotion of Science and Technology in Okayama Prefecture by the Ministry of Education, Culture, Sports, Science and Technology of Japan.

References

Abarzua F, Sakaguchi M, Takaishi M, Nasu Y, Kurose K, Ebara S, Miyazaki M, Namba M, Kumon H, Huh NH (2005) Adenovirus-mediated overexpression of REIC/Dkk-3 selectively induces apoptosis in human prostate cancer cells through activation of c-Jun-NH2-kinase. Cancer Res 65: 9617–9622

Bafico A, Liu G, Yaniv A, Gazit A, Aaronson SA (2001) Novel mechanism of Wnt signalling inhibition mediated by Dickkopf-1 interaction with LRP6/Arrow. Nat Cell Biol 7: 683-686

Bamberger C, Hafner A, Schmale H, Werner S (2005) Expression of different p63 variants in healing skin wounds suggests a role of p63 in reepithelialization and muscle repair. Wound Repair Regen 13: 41-50

Barrantes IB, Montero-Pedrazuela A, Guadaño-Ferraz A, Obregon MJ, Martinez de MR, Gailus-Durner V, Fuchs H, Franz TJ, Kalaydjiev S, Klempt M, Hölter S, Rathkolb B, Reinhard C, Morreale de EG, Bernal J, Busch DH, Wurst W, Wolf E, Schulz H, Shtrom S, Greiner E, Hrabé de AM, Westphal H, Niehrs C (2006) Generation and characterization of dickkopf3 mutant mice. Mol Cell Biol 26: 2317-2326

Byun T, Karimi M, Marsh JL, Milovanovic T, Lin F, Holcombe RF (2005) Expression of secreted Wnt antagonists in gastrointestinal tissues: potential role in stem cell

homeostasis. J Clin Pathol 58: 515-519

Das DS, Wadhwa N, Kunj N, Sarda K, Pradhan BS, Majumdar SS (2013) Dickkopf homolog 3 (DKK3) plays a crucial role upstream of Wnt/b-catenin signaling for Sertoli cell mediated regulation of spermatogenesis. PLoS One 8: e63603. doi:10.1371/journal.pone.0063603

Du G, Kataoka K, Sakaguchi M, Abarzua F, Than SS, Sonegawa H, Makino T, Shimizu T, Huh NH (2011) Expression of REIC/Dkk3 in normal and hyperproliferative epidermis. Exp Dermatol 20: 273-277

Fujii Y, Hoshino T, Kumon, H (2014) Molecular simulation analysis of the structure complex of C2 domains of DKK family members and β-propeller domains of LRP5/6: explaining why DKK3 does not bind to LRP5/6. Acta Med Okayama 68: 63-78

Glinka A, Wu W, Delius H, Monaghan AP, Blumenstock C, Niehrs C (1998) Dickkopf-1 is a member of a new family of secreted proteins and functions in head induction. Nature 391: 357-362

Hara K, Kageji T, Mizobuchi Y, Kitazato KT, Okazaki T, Fujihara T, Nakajima K, Mure H, Kuwayama K, Hara T Nagahiro S (2015) Blocking of the interaction between Wnt proteins and their co-receptors contributes to the anti-tumor effects of

adenovirus-mediated Dkk3 in glioblastoma. Cancer Lett 356: 496-505

Kataoka K, Du G, Maehara N, Murata H, Sakaguchi M Huh N (2012) Expression pattern of REIC/Dkk3 in mouse squamous epithelia. Clin Exp Dermatol 37: 428-431

Krupnik VE, Sharp JD, Jiang C, Robison K, Chickering TW, Amaravadi L, Brown DE, Guyot D. Mays G, Leiby K, Chang B, Duong T, Goodearl AD, Gearing DP, Sokol SY, McCarthy SA (1999) Functional and structural diversity of the human Dickkopf gene family. Gene 238: 301-313

Lee EJ, Jo M, Rho SB, Park K, Yoo YN, Park J, Chae M, Zhang W, Lee JH (2009) Dkk3, downregulated in cervical cancer, functions as a negative regulator of beta-catenin. Int J Cancer 124: 287-297

Mao B and Niehrs C (2003) Kremen2 modulates Dickkopf2 activity during Wnt/LRP6 signaling. Gene 302: 179-183

Monaghan AP, Kioschis P, Wu W, Zuniga A, Bock D, Poustka A, Delius H Niehrs C (1999) Dickkopf genes are co-ordinately expressed in mesodermal lineages. Mech Dev 87: 45-56

Niehrs C (2006) Function and biological roles of the Dickkopf family of Wnt modulators. Oncogene 57: 7469-7481

Ochiai K, Watanabe M, Ueki H, Huang P, Fujii Y, Nasu Y, Noguchi H, Hirata T,

Sakaguchi M, Huh NH, Kashiwakura Y, Kaku H, Kumon H (2011) Tumor suppressor REIC/Dkk3 interacts with the dynein light chain, Tctex-1. Biochem Biophys Res Commun 412: 391-395

Papatriantafyllou M, Moldenhauer G, Ludwig J, Tafuri A, Garbi N, Hollmann G, Küblbeck G, Klevenz A, Schmitt S, Pougialis G, Niehrs C, Gröne HJ, Hämmerling GJ, Arnold B, Oelert T (2012) Dickkopf-3, an immune modulator in peripheral CD8 T-cell tolerance. Proc Natl Acad Sci USA 109: 1631-1636

Schaeren-Wiemers N and Gerfin-Moser A (1993) A single protocol to detect transcripts of various types and expression levels in neural tissue and cultured cells: in situ hybridization using digoxigenin-labelled cRNA probes. Histochemistry 100: 431-440

Suwa T, Chen M, Hawks CL, Hornsby PJ (2003) Zonal expression of dickkopf-3 and components of the Wnt signalling pathways in the human adrenal cortex. J Endocrinol 178: 149-158

Tanimoto R, Abarzua F, Sakaguchi M, Takaishi M, Nasu Y, Kumon H, Huh NH (2007) REIC/Dkk3 as a potential gene therapeutic agent against human testicular cancer. Int J Mol Med 19: 363-368

Tanimoto R, Sakaguchi M, Abarzua F, Kataoka K, Kurose K, Murata H, Nasu Y, Kumon H, Huh NH (2010) Down-regulation of BiP/GRP78 sensitizes resistant

prostate cancer cells to gene-therapeutic overexpression of REIC/Dkk3. Int J Cancer 126: 1562–1569

Tsuji T, Miyazaki M, Sakaguchi M, Inoue Y, Namba M (2000) A REIC gene shows down-regulation in human immortalized cells and human tumor-derived cell lines. Biochem Biophys Res Commun 268: 20-24

Veeck J, Wild PJ, Fuchs T, Schüffler PJ, Hartmann A, Knüchel R, Dahl E (2009) Prognostic relevance of Wnt-inhibitory factor-1 (WIF1) and Dickkopf-3 (DKK3) promoter methylation in human breast cancer. BMC Cancer 9: 217. doi:10.1186/1471-2407-9-217

Veeck J and Dahl E (2012) Targeting the Wnt pathway in cancer: the emerging role of Dickkopf-3. Biochim Biophys Acta 1825: 18-28

Wang Z, Ma LJ, Kang Y, Li X, Zhang XJ (2015) Dickkopf-3 (Dkk3) induces apoptosis in cisplatin-resistant lung adenocarcinoma cells via the Wnt/β-catenin pathway. Oncol Rep 33: 1097-1106

Watanabe M, Kashiwakura Y, Huang P, Ochiai K, Futami J, Li SA, Takaoka M, Nasu Y, Sakaguchi M, Huh NH, Kumon H (2009) Immunological aspects of REIC/Dkk3 in monocyte differentiation and tumor regression. Int J Oncol 34: 657-663

Xiang T, Li L, Yin X, Zhong L, Peng W, Qiu Z, Ren G, Tao Q (2013) Epigenetic

silencing of the WNT antagonist Dickkopf 3 disrupts normal Wnt/ β-catenin signalling and apoptosis regulation in breast cancer cells. J Cell Mol Med 10: 1236-1246

Figure legends

Fig. 1 ISH of mouse stomach and duodenum to detect *Dkk3* mRNA. Longitudinal sections of the stomach (**a, b**), forestomach (**c-f**), gastric corpus (**g-m**), pylorus (**n-q**), and duodenum (**r-u**) were hybridized with antisense (**a, c, d, g, h, k, m, n, o, r, s**) and sense (**b, e, f, i, j, p, q, t, u**) probes. The open square outlines shown in panel (**a**) represent the areas that are shown as magnified views in (**c, g, n, r**), respectively. Panels (**d, h, o, s**) are magnified views of an area in panels (**d, h, o, s**), respectively. The panels for sense probes are shown in the same way. (**l, m**) Localization of lectin GSII is shown in red. (**m**) Merged view of (**k**) and (**l**). BG: Brunner's glands; CCL: chief cell layer; GP: gastric pits; IV: intestinal villi; MsL: muscle layer; PCL: parietal cell layer; PG; pyloric glands; SSEp: stratified squamous epithelium. *Scale bars*; 100 μm

Fig. 2 ISH of mouse gallbladder and intestines to detect *Dkk3* mRNA. Gallbladder (**a-d**), small intestine (**e-h**), colon (**i-l**), and rectum (**m-p**) sections were hybridized with antisense and sense probes as indicated. Panels (**b, f, j, n**) are magnified views of an area in panels (**a, e, i, m**), respectively. The panels for sense probes are shown in the same way. GC: goblet cells; IG: intestinal glands; IV: intestinal villi; LIG: large intestinal glands; McL: mucosal layer; MsL: muscle layer. *Scale bars*; 100 μm

Fig. 3 ISH of mouse lymphatic organs to detect *Dkk3* mRNA. Spleen (**a-d**), thymus (**e-h**), and lymph node (**i-l**) sections were hybridized with antisense and sense probes as indicated. The open square outlines shown in the first and third columns represent the areas that are shown as magnified views in the second and fourth columns. Cor: cortex; Med: medulla; RP: red pulp; WP: white pulp. *Scale bars*; 100 μm

Fig. 4 ISH of mouse reproductive organs to detect *Dkk3* mRNA. Testis (**a-f**), dorsal prostate gland (**g-i**), seminal vesicle (**j-l**), ovary (**m-o**), and uterus (**p-r**) sections were hybridized with antisense (**a, b, d, f, g, h, j, k, m, n, p, q**) and sense (**c, i, l, o, r**) probes. (**e, f**) Localization of Vimentin is shown in green. (**f**) Merged view of (**d**) and (**e**). Ant: antrum; BM: basement membrane; CT: connective tissue; Em: endometrium; Ep: epithelium; Mm: myometrium; O: oocyte; S: stroma; SeT: seminiferous tubule; SG: stratum granulosum; SM: smooth muscle; SZ: spematozoa; TCC: tall columnar cells; TF: theca folliculi. *Scale bars*; 25 μm in (**d-f**); 100 μm in other panels

Fig. 5 Western blotting of Dkk3 in mouse various tissues. Expression of Dkk3 protein in wild-type (WT) and *Dkk3* knockout (KO) mouse brain, eye, heart, stomach, adrenal

gland, skin, testis, and spleen is shown. The bracket indicates a heterogeneous set of bands ranging from 38 to 65 kDa detected in the wild-type brain, eye, heart, stomach, adrenal, and skin extracts, and these bands were not detected in the equivalent tissues from the KO mice. In the testis and spleen, however, multiple bands below 50 kDa were detected even in the extracts from the KO mice. Western blot analysis of Cyclophilin B (20 kDa in most tissues; 25 kDa in eye extract) and CBB staining verifies that the same amount of proteins was loaded in each lane and processed for Western blot analysis. In the skin, Cyclophilin B is not expressed

Fig. 6 Fluorescent immunostaining of mouse nervous system, heart, and adrenal gland. Hippocampus and cortex levels of the brain (**a-d** and **e-h**, respectively), as well as retinal (**i-l**), heart (**m-p**), and adrenal (**q-t**) tissue sections, from wild-type and knockout mice (as indicated) were subjected to fluorescent immunostaining with a Dkk3 antibody (green) and DAPI staining of nuclei (blue). (**a-l, q-t**) The open square outlines shown in the first and third columns represent the areas that are shown as magnified views in the second and fourth columns. Similarly, panels **n** and **p** represent a magnified view of the outlined area shown in panels **m** and **o**, respectively. (**q-t)** The adrenal medulla was labeled with anti-TH antibody (shown in red). (**q, r**) Merged image to indicate

colocalization of Dkk3 (green) and TH (red) proteins. CA1: hippocampus CA1 region; CC: cerebral cortex; Cor: cortex; GCL: ganglion cell layer; INL: inner nuclear layer; LHA: left heart atrium; LHV: left heart ventricle; Med: medulla; RHA: right heart atrium; RHV: right heart ventricle. *Scale bars*; 100 μm

Fig. 7 Fluorescent immunostaining of mouse gastrointestinal tract and skin. Longitudinal sections of stomach (**a, b**), forestomach (**c-f**), gastric corpus (**g-j**), pylorus (**k-n**), intestine (**o-r**), and skin (**s-x**) tissue sections from wild-type and knockout mice (as indicated) were subjected to fluorescent immunostaining with a Dkk3 antibody (green) and DAPI staining of nuclei (blue). The stomach and intestine sections were also stained with an anti-smooth muscle actin (SMA) antibody (red). For panels **c-r**, the open square outlines shown in the first and third columns represent the areas that are shown as magnified views in the second and fourth columns. (**s, v**) Skin and underlying abdominal muscle tissues from wild-type and knockout mice are shown, respectively. Magnified views of the skin and underlying striated muscle in panels **s** and **v** are shown in panels **t**, **u** and **w**, **x**, respectively. CCL: chief cell layer; epi: epidermis; der: dermis; GP: gastric pits; hf: hair follicle; IG: intestinal glands; MsL: muscle layer; PCL: parietal cell layer; SSEp: stratified squamous epithelium; IV: intestinal villi. *Scale bars*; 100 μm

Supplementary material

Expression analysis of *Dickkopf-related protein 3* (*Dkk3)* suggests its pleiotropic roles for a secretory glycoprotein in adult mouse

Junji Inoue[1] ▪ Hirofumi Fujita[1] ▪ Tetsuya Bando[1] ▪ Yoichi Kondo[1,†] ▪ Hiromi Kumon[2,3] ▪ Hideyo Ohuchi[1]

[1] Department of Cytology and Histology, Okayama University Graduate School of Medicine, Dentistry and Pharmaceutical Sciences, 2-5-1 Shikata-cho, Kita-ku, Okayama 700-8558, Japan

[2] Innovation Center Okayama for Nanobio-targeted Therapy (ICONT), Okayama University, 2-5-1 Shikata-cho, Kita-ku, Okayama 700-8558, Japan

[3] Niimi College, 1263-2 Nishigata, Niimi, Okayama 718-8585, Japan

Table S1. Antibodies and reagents used in the present study

Name of Antibody/Reagent	Supplier/Vender	Catalog/Clone #	Antibody Registry[a]	Dilution
Anti-Actin, alpha-Smooth Muscle	Sigma-Aldrich	A2547, clone 1A4	AB_476701	500(I)[b]
Anti-Cyclophilin B	Cell Signaling Technology	79652		1000(W)[c]
Anti-Dkk3				1000(I), 10000(W
Anti-Tyrosine Hydroxylase	Millipore	MAB318, clone LNC1	AB_10050306	250(I)
Anti-PNMT	Enzo Life Sciences	BML-PZ1040	AB_2167779	500(I)
Anti-Vimentin[d]	Sigma-Aldrich	V5255, clone VIM-13.2	AB_477625	100(I)
Alexa Fluor 488 anti-rabbit IgG	Thermo Fisher Scientific	A11034	AB_257621	750(I)
Alexa Fluor 488 anti-mouse IgM	Thermo Fisher Scientific	A21042	AB_141357	500(I)
Alexa Fluor 594 anti-mouse IgG	Thermo Fisher Scientific	A11032	AB_141672	750(I)
Alexa Fluor 594 GSII[e]	Thermo Fisher Scientific	L21416		

[a] http://antibodyregistry.org/, [b] I: Immunohistochemistry, [c] W: Western blotting

References:[d] Tanemura K et al. (1994) Tissue Cell 26; 447-455. [e] Ramsey VG et al. (2007) Development 134; 211-222.

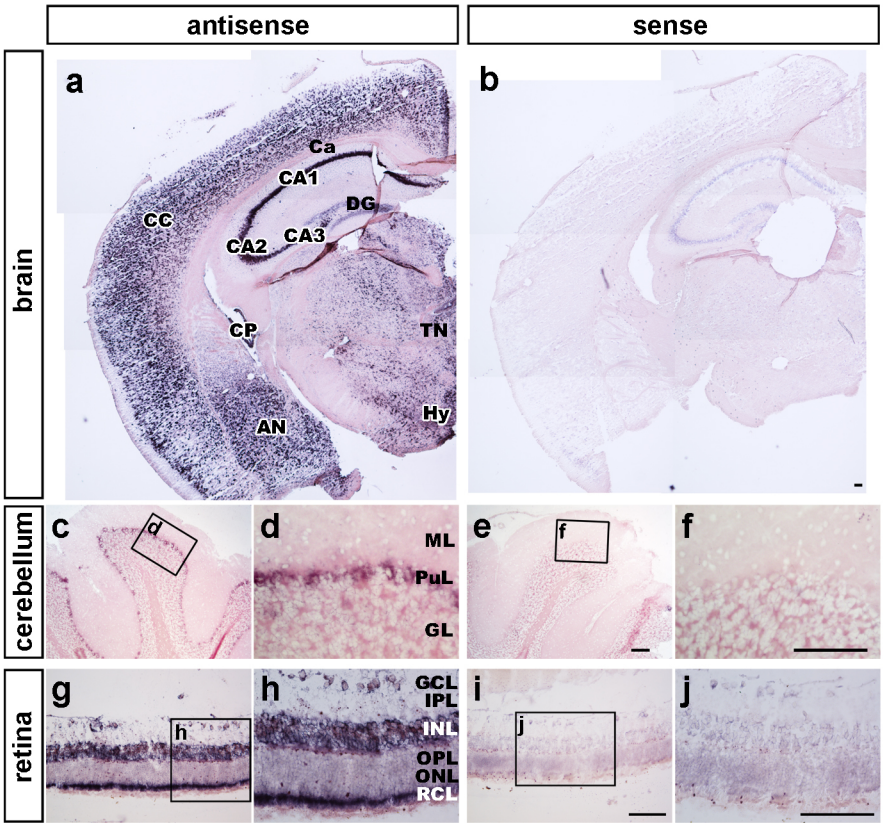

Fig. S1. ISH of mouse brain and retina to detect *Dkk3* mRNA .

Coronal sections from the hippocampal (1.82 mm caudal to bregma) (**a, b**) and cerebellum (6.12 mm caudal to bregma) (**c-f**) levels of the brain, as well as retina sections (**g-j**), were hybridized with antisense and sense probes as indicated. The open square outlines shown in panels **c, e, g,** and **i** are shown as magnified views in panels **d, f, h,** and **j,** respectively. Scale bars: 100 μm. AN: amygdaloid nucleus; Ca: callosum; CA1: hippocampus CA1 region; CA2: hippocampus CA2 region; CA3: hippocampus CA3 region; CC: cerebral cortex; CP: choroid plexus; DG: hippocampus dentate gyrus; GCL: ganglion cell layer; GL: granular layer; Hy: hypothalamus; INL: inner nuclear layer; IPL: inner plexiform layer; ML: molecular layer; ONL: outer nuclear layer; OPL: outer plexiform layer; PuL: Purkinje cell layer; RCL: layer of rods and cones; TN: thalamic nucleus.

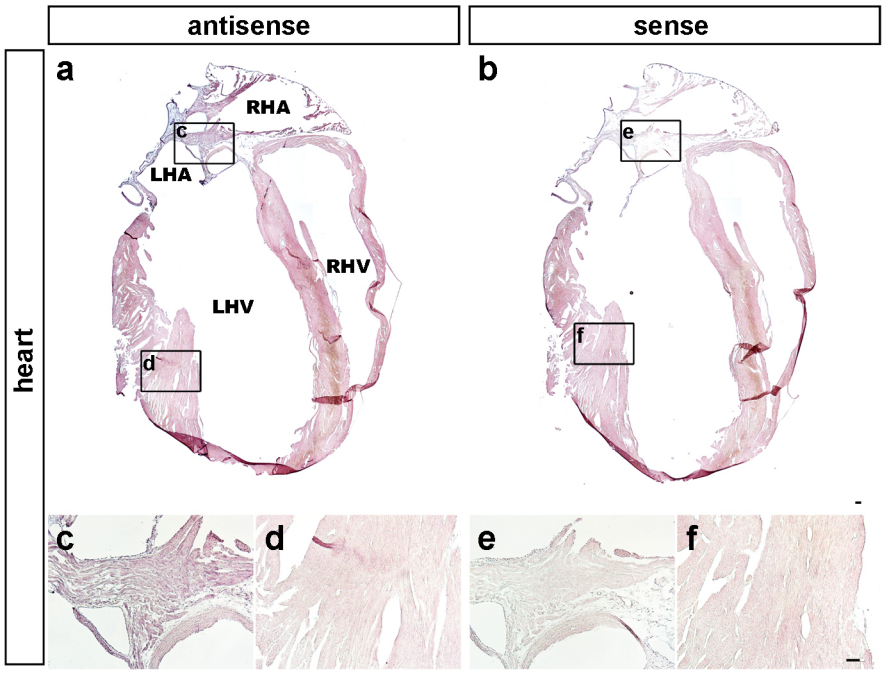

Fig. S2. ISH of mouse heart to detect *Dkk3* mRNA.
(a, b) Coronal sections of the heart were hybridized with antisense and sense probes, respectively. (**c, d**) Magnified views of the atrium and heart ventricles from panel **a**. (**e, f**) Magnified views of the atrium and ventricles from panel **b**. Scale bars: 100 μm. LHA: left heart atrium; LHV: left heart ventricle; RHA: right heart atrium; RHV: right heart ventricle.

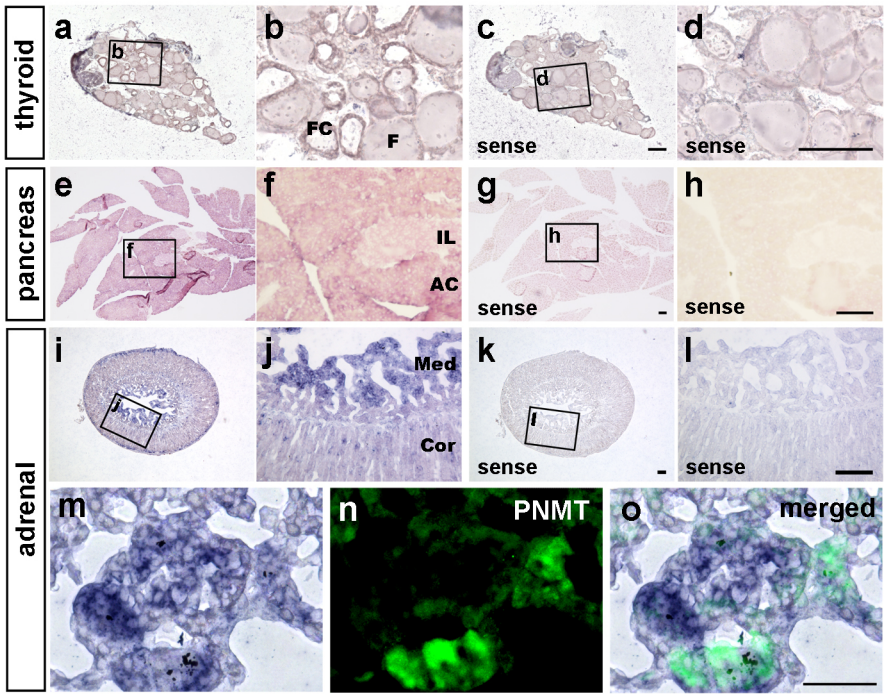

Fig. S3. ISH of mouse endocrine tissues to detect *Dkk3* mRNA.
Thyroid (**a-d**), pancreas (**e-h**), and adrenal gland (**i-o**) sections were hybridized with antisense (**a, b, e, f, i, j, m, o**) and sense (**c, d, g, h, k, l**) probes. The open square outlines shown in the first and third columns represent the areas that are shown as magnified views in the second and fourth columns, and are labeled accordingly. (**m-o**) Magnified views of the medullar cells, where high level of *Dkk3* expression is shown in intense blue (**m**), localization of Phenylethanolamine N-methyltransferase (PNMT) is shown in green fluorescence (**n**), and merged view of (**m**) and (**n**) is shown in (**o**). Note that intense signal for *Dkk3* mRNA is detected in the cells devoid of green florescence. Scale bars: 100 μm in (**a-l**), 50 μm in (**m-o**). AC: acinus; Cor: cortex; F: follicle; FC: follicular cells; IL: islet of Langerhans; Med: medulla.

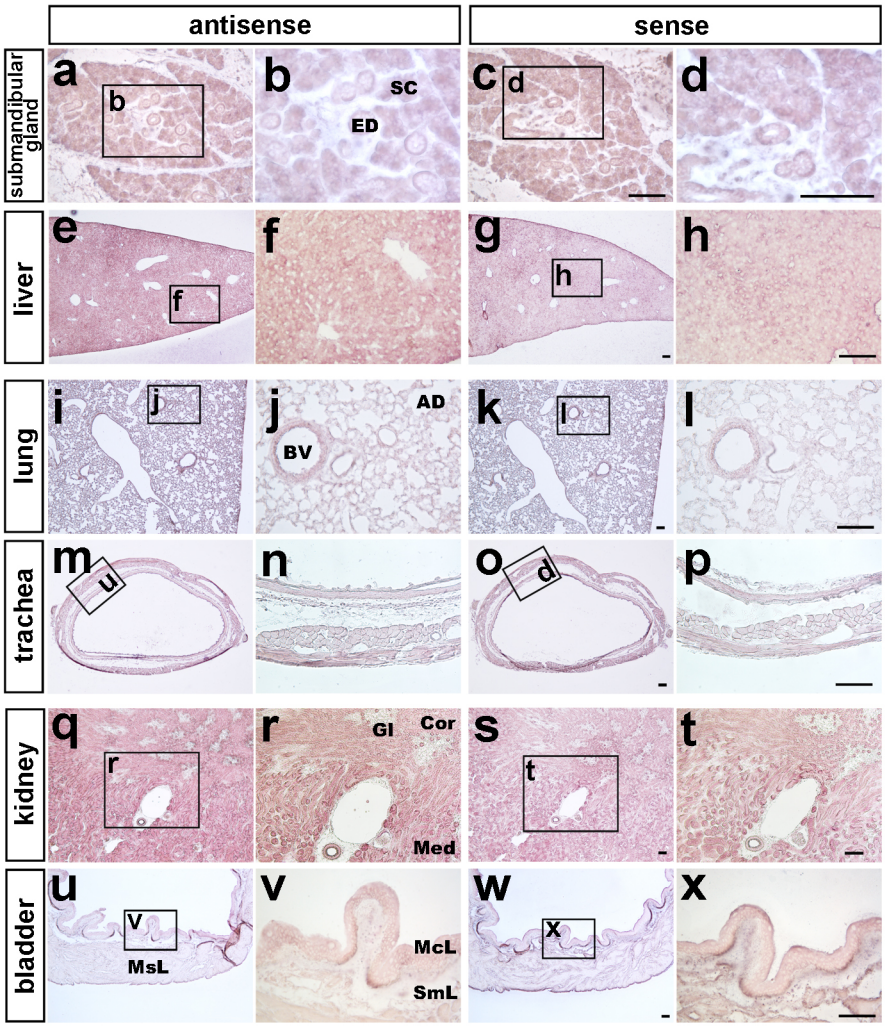

Fig. S4. ISH of mouse digestive glands, respiratory organs, and urinary organs to detect *Dkk3* mRNA. Tissue sections of the submandibular gland, liver, lung, trachea, kidney, and bladder were hybridized with antisense and sense probes as indicated. The open square outlines shown in the first and third columns represent the areas that are shown as magnified views in the second and fourth columns. Scale bars: 100 μm. AD: alveolar duct; BV: blood vessel; Cor: cortex; ED: excretory duct; Gl: glomeruli; McL: mucosal layer; Med: medulla; MsL: muscle layer; SC: serous cells; SmL: submucosal layer.

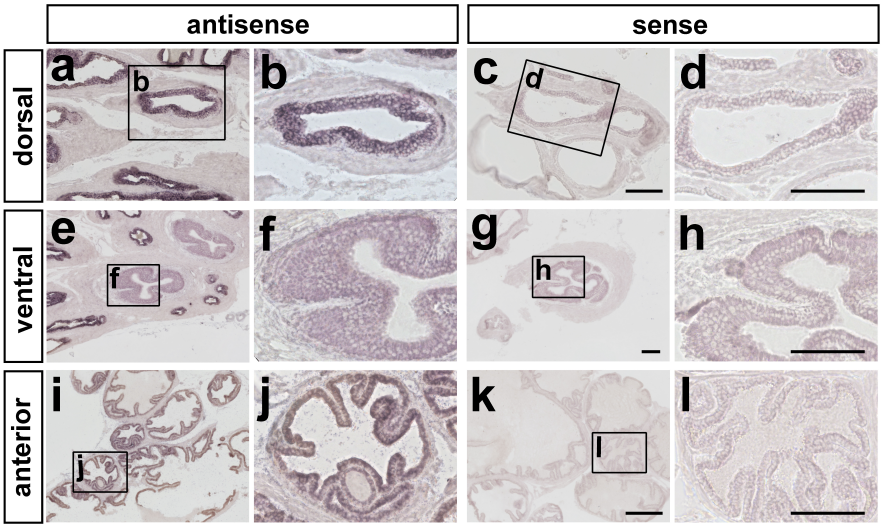

Fig. S5. ISH of mouse prostate glands to detect *Dkk3* mRNA. Tissue sections of dorsal, ventral, and anterior prostate glands were hybridized with antisense and sense probes as indicated. The open square outlines shown in the first and third columns represent the areas that are shown as magnified views in the panels in the second and fourth columns. Scale bars: 100 μm.

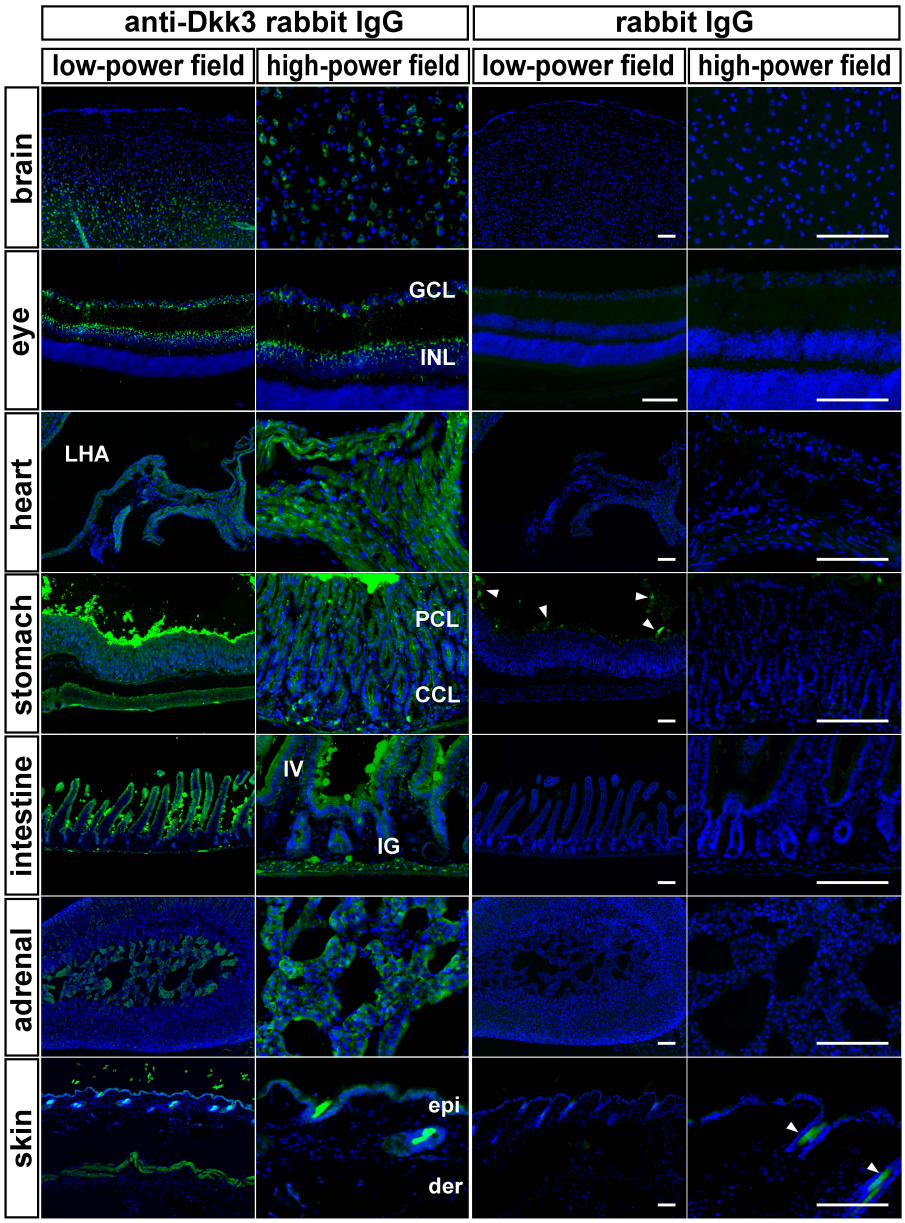

Fig. S6. Control rabbit IgG gave essentially no fluorescent signals in brain, eye, heart, stomach, intestine, adrenal, or skin except small amount of fluorescence in the cavity of stomach, and hair follicles (arrowheads). Scale bars: 100 μm. GCL: ganglion cell layer; INL: inner nuclear layer; PCL: parietal cell layer; CCL: chief cell layer; LHA: left heart atrium; IV: intestinal villi; IG: intestinal glands; epi: epidermis; der: dermis.